Radiation Measurements 139 (2020) 106488

Contents lists available at ScienceDirect

Radiation Measurements

journal homepage: www.elsevier.com/locate/radmeas

# A distributed and interconnected network of sensors for environmental radiological monitoring

L. Gallego Manzano [a,*], C. Bisegni [b], H. Boukabache [a], A. Curioni [a,1], N. Heracleous [a], F. Murtas [b], D. Perrin [a], M. Silari [a]

[a] CERN, 1211 Geneva 23, Switzerland
[b] Frascati National Laboratories, INFN, 00044 Frascati, Italy

ARTICLE INFO

*Keywords:*
Radioactive waste monitoring
Internet of Things
LoRa
Environmental radiation monitoring

ABSTRACT

The W-MON project aims to improve and automatize the control of the presence of radioactive material in conventional waste containers at CERN using a distributed network of interconnected low-power radiation sensors. The key development is the integration of a lightweight but sensitive radiation sensor in a powerful network that allows continuous data recording, transfer and storage in a database for alarm triggering and subsequent data analysis. The Chiyoda D-shuttle personal dosimeter was used as proof-of-concept. Extensive tests performed with the commercial version of the D-shuttle showed that its robustness, stability under variable thermal conditions, high sensitivity and hourly dose logging capabilities make it a strong candidate for the project. To comply with the requirements of remote operation and wireless data transmission to a central server, a customized version of the D-shuttle has been developed. Two additional radiation sensors are also currently being considered. The sensors have been coupled to a custom-made communication board allowing for long-range low-power LoRa wireless data transmission. A centralized IoT (Internet of Things) end-to-end data architecture has been developed for real-time monitoring and visualization of the radiation level in waste containers before the final integration into REMUS, the overall CERN Radiation and Environment Monitoring Unified Supervision service.

## 1. Introduction

In a complex working environment such as CERN, radiation safety is both a key concern and a challenge. Detectors for prompt radiation monitoring, measurements of residual radioactivity, and personal dosimetry are essential tools to control exposure to ionizing radiation. In particular, to prevent potential accidental releases of radioactive material outside CERN, multi-level periodical radiological controls of conventional waste are carried out prior to final disposal from the CERN sites.

Ideally, a reliable and efficient radiological control of conventional waste requires continuous and homogeneous monitoring. The current first-level monitoring procedure consists in the manual control of waste containers by a radiation protection technician equipped with a hand-held radiation survey meter. The controls are performed over more than two hundred household containers for ordinary waste located outside buildings where there is a potential risk that radioactive material is dumped by mistake (e.g. close to accelerator access points). This implies containers spread-out over a wide area covering hundreds of hectares. The containers are located outdoors and are regularly emptied through the standard garbage collection procedure imposing stringent requirements on the design of the radiation devices in terms of robustness, reliability, energy efficiency, security, and network coverage. Requirements of an automated monitoring system are listed in Table 1.

Based on the reports of the trained operators performing the monitoring, the majority of items that tested positive were small metal parts, such as bolts and nuts or filing from machining. Therefore, the type of radiation to be monitored is mainly gamma rays with sensitivity down to the natural background level (typically 0.1 μSv/h).

The containers are located outdoors and are exposed to variable weather conditions. They are emptied at least twice per week by being flipped over with severe vibrations and shocks. Therefore, the radiation sensors need to withstand such adverse conditions without loss of sensitivity or degradation of performance. Continuous data recording and transfer will improve not only the quality of the data but also the efficiency of the system. However, an autonomous network of interconnected devices must require minimal, quick, and cost-effective

* Corresponding author.
*E-mail address:* lucia.gallego.manzano@cern.ch (L. Gallego Manzano).
[1] Now with BAQ Sàrl, Rue des Pâquis 11, 1201 Geneva, Switzerland.

https://doi.org/10.1016/j.radmeas.2020.106488
Received 13 July 2020; Received in revised form 28 October 2020; Accepted 4 November 2020
Available online 10 November 2020

**Table 1**
Requirements of an automated system to monitor radioactivity in waste.

| Feature | Description | W-MON requirements |
|---|---|---|
| Sensitivity | Sensitivity to gamma radiation | Sensitivity to a dose rate down to 100 nSv/h (i.e. average natural radiation background) |
| Data rate | Data acquisition rate | Continuous data recording |
| Data transfer | Data transmission protocol | Wireless real-time data transmission (i.e. 3G/4G, Bluetooth, WiFi or LoRa) |
| Robustness | Resistance to severe weather conditions vibrations and mechanical shocks | −20 °C to +50 °C and IP68 protection |
| Reliability | Maintenance and system autonomy | Battery powered devices with real-time system operation with minimum maintenance over several years |
| Data management | Data logging, data analysis and data sharing | Web-service platform with top-level functionalities |
| Versatility | Flexible design | Easy adaptation to different applications |
| Cost | Cost-effectiveness | Acceptable cost per device including maintenance |

maintenance. Thus, radiation sensors need to be battery powered and should run on relatively small batteries for several years. On this basis, ultra-low-power consumption is one of the most crucial requirements.

The goal of the W-MON (Waste radiation MONitoring) project is to design, build, test, and deploy a network of radiation sensors for real-time monitoring of waste. This network is being designed to connect one thousand or more devices located across the different CERN sites and integrate them into REMUS, the CERN Radiation and Environment Monitoring Unified Supervision service (Ledeul et al., 2015). The objectives of this papers are (1) to provide a detailed examination of the key aspects of the project, (2) to present the proof of concept of the system demonstrating technology capabilities, and (3) introduce the developments in a customized solution for the radiation monitoring devices.

## 2. Materials and methods

### 2.1. The D-shuttle personal dosimeter

The radiation sensors measure and transmit the radiation level in the containers. These devices should consist of a gamma radiation sensor with a high sensitivity down to the natural background level, a micro-controller, specifically designed hardware for wireless data transmission and communication, an efficient antenna for wireless communication, and a shock sensor to avoid spurious signals.

As a promising option for the radiation sensor, we identified the D-shuttle[2] personal dosimeter developed by the National Institute of Advanced Industrial Science and Technology (AIST) and Chiyoda Technol Corporation. The D-shuttle is a small (68 mm × 32 mm × 14 mm) and lightweight device (23 g) based on a Hamamatsu Si diode originally developed for individual dosimetry of the residents of the Fukushima Prefecture after the nuclear power plant accident in 2011. The dosimeter is battery-powered by a coin-type lithium battery ensuring one year of autonomy (assuming two readings per day). The hourly personal dose equivalent (Hp(10)) and the total cumulative dose in the range from 0.1 μSv to 99.9999 mSv are stored in the on-board memory providing time-stamped measurements for up to 400 days. It also embeds an alarm system for high dose, electromagnetic shielding, and a shock sensor to remove spurious counts. The D-shuttle was calibrated with a Cs-137 source ensuring a dose rate linearity better than 10% in the range from 2 μSv/h to 3 mSv/h (Musto et al., 2019; Kim et al., 2019; Naito et al., 2016). The dosimeter energy response for gamma rays is ±30% (response relative to Co-60) in the energy range between 60 keV and 1.25 MeV (Musto et al., 2019; Cemusová et al., 2017). The D-shuttle is supplied with a stand-alone, small and lightweight personal reader that provides the dose received in the last 24 h and the total integrated dose from the time it was reset. A more sophisticated reader connected to a PC through an USB cable gives access to the D-shuttle memory with the full hourly, monthly, and yearly dose record.

Even if the D-shuttle does not provide long-range wireless capabilities, its performance in terms of sensitivity, stability, robustness, and dose rate logging capacities makes it a strong candidate for proof-of-concept. The characteristics of the D-shuttle as a personal dosimeter for members of the public have been extensively tested by various authors (Musto et al., 2019; Kim et al., 2019; Adachi et al., 2015; Islam et al., 2019) and its suitability for stable low-dose rate conditions has been reported (Cemusová et al., 2017). Extensive performance tests carried out with the D-shuttle using a standard metallic waste container and typical radioactive waste are presented in Section 4.1. Background measurements over a seven month period showed that the dosimeters are stable, even under variable thermal conditions, demonstrating a high-enough sensitivity for this particular application with a mean background dose rate of 0.07 ± 0.03 μSv/h (see Section 4.1.2).

### 2.2. Other radiation sensors

The commercial version of the D-shuttle personal dosimeter was used to prove the potential of the W-MON project. However, one of the key points of the W-MON system is the integration of the sensors in a distributed network allowing for remote operation and long-range wireless data transmission to a central server. The D-shuttle has two independent communication interfaces for data transfer associated to the two different readers: an optical link and a wireless technology based on an ultra-low-power 2.5 GHz RF transceiver. None of them are suitable for long-range distance data transmissions. Consequently, one of the adopted options was to developed a modified version of the D-shuttle based on the specific needs of the W-MON project in collaboration with AIST. The new customized version maintains the original features of the D-shuttle (see Table 2), but it is specifically designed to be easily coupled to a communication board that provides low power consumption (30% lower than the standard D-shuttle personal dosimeter) and longer-range wireless communication. In addition to the customized version of the D-shuttle, two other gamma radiation sensors provided by two different vendors have been considered. The objective is to compare the performance of the three sensors not only in terms of sensitivity and reliability, but also in terms of cost-effectiveness, scalability, long-term component availability, and lifetime expectancy. The two radiation sensors are: the BG51,[3] developed by Teviso Technologies and manufactured in Switzerland and the NI-RM02,[4] developed by Nuclear Instruments (NI) based on a First Sensor[5] Si PIN diode and manufactured in Italy . The technical specifications of the three sensors (Fig. 1) as provided by the manufacturers are listed in Table 2.

[2] D-shuttle: http://www.c-technol.co.jp/eng/e-dshuttle, (accessed 22 June 2020).

[3] BG51: https://www.teviso.com/file/pdf/bg51-data-specification.pdf, (accessed 22 June 2020).

[4] Nuclear Instruments NI-RM02, Private communication.

[5] First Sensor: https://www.first-sensor.com/cms/upload/datasheets/X100-7_THD_5000040.pdf, (accessed 22 June 2020).


(a) (b) (c)

**Fig. 1.** (a) Top view of the customized D-shuttle dosimeter, (b) the Teviso BG51 radiation sensor and (c) the Nuclear Instrument sensor board.

**Table 2**
Technical specifications as provided by the manufacturers of the three candidates as radiation sensor for the W-MON project.

| Feature | D-shuttle[a] | BG51 | NI-RM02 |
|---|---|---|---|
| Type of sensor | Hamamatsu Si PIN diode | Array of customized Si PIN diodes | First sensor Si PIN diode |
| Sensor size | 7.29 $mm^2$ | 15.5 $mm^2$ | 100 $mm^2$ |
| Measurement range | 0.1 μSv/h to 99.9999 mSv/h | 0.1 μSv/h to 100 mSv/h | 0.01 μSv/h to 300 μSv/h |
| Energy response | 60 keV to 1.25 MeV | 50 KeV to >2 MeV | 50 KeV to 2 MeV |
| Pulse count rate | 1.7 cpm for 1 μSv/h dose rate for Cs-137 | 5 cpm ± 15% for 1 μSv/h dose rate for Cs-137 and Co-60 | 50 cpm ± 15% for 1 μSv/h dose rate for Cs-137 |
| Operational temperature | −20 °C to >40 °C | −30 °C to 60 °C | −20 °C to 50 °C |
| Output signal | SPI or asynchronous serial communication | TTL signal | TTL signal |
| Embedded shock sensor | Yes | No | Yes |

[a]Technical specifications of the commercial version of the D-shuttle personal dosimeter.

## 3. W-MON IoT infrastructure

Fig. 2 shows a simplified sketch of the W-MON infrastructure. The depicted end-devices, or nodes, represent the set of monitoring units that include an array of small and smart radiation sensors coupled with specifically designed hardware for wireless data transmission and communication. Apart from the radiation sensors, the totality of the W-MON network consists of gateways, network services, a database to store the data, and the application servers.

Due to the large number of devices and the scale of the deployment, the technology used for the W-MON connectivity needs not only to provide wide coverage, but also robust signals able to penetrate buildings and co-exist with many other devices without interference or signal collisions. The devices must operate for long periods of time on small power sources with minimal maintenance, while transmitting periodically and wirelessly small amounts of data to the server. Therefore, the technology for communication and data transfer needs to be energy-efficient to enable long battery lifetime, reducing the need of battery replacement and the cost per device. Moreover, to guarantee full coverage of all CERN sites, a wireless network based on a long-range technology is required.

Data transmission and communication from the monitoring system to the monitoring service is achieved via a Low Power Wide Area Networks (LPWAN) technology (Raza et al., 2017; Moyer, 2015) and in particular, via LoRa, which provides long-range low-power wireless communication and has a line-of-sight range of around 2 km in dense urban areas and up to 15 km in rural areas (see LoRa Alliance, 2020; Augustin et al., 2016; Petäjäjärvi et al., 2017; Bezerra et al., 2019). Apart from ultra-low-power communication and wide coverage, network scalability, i.e. number of end-devices per gateway, is also of crucial importance. LoRa is designed to potentially serve millions of devices operating at low data rates, which is particularly appealing for Internet of Things (IoT) applications (Gnawali et al., 2016). Accordingly, we have developed a robust and efficient centralized IoT end-to-end data pipeline that relies on state-of-the-art open source technologies (see Fig. 3). W-MON utilizes the new CERN LPWAN network based on LoRaWAN (Sierra, 2019), which uses MQTT (Message Queuing Telemetry Transport) protocol for communication and ensures a secure data flow across the network. The radiation sensors are coupled to a custom-made communication board with specifically designed hardware and firmware allowing for long-range low-power LoRa data transmission. Data from the radiation sensors are periodically sent, collected and stored in a centralized database system provided by CERN based on Kafka[6] for real-time data streaming and InfluxDB[7] for data storage. A set of customized user dashboards was created using Grafana[8] for real-time monitoring, data visualization, and status control of the devices. The new W-MON data infrastructure is a reliable and highly scalable monitoring architecture, designed to ensure and facilitate the final integration of the system into REMUS.

## 4. Results and discussion

### 4.1. Feasibility tests under real operational conditions

A set of tests under real operational conditions were performed using the commercial version of the D-shuttle with manual reading of the dose. The dosimeters were mounted on a regular-use metallic container for conventional waste (see Fig. 4) and the hourly dose was obtained from the recorded data using the PC interface. Different configurations with ten and eight sensors around the container placed at different positions were studied. The goal of these tests was to assess the suitability of the sensors to measure weakly radioactive waste as well as to evaluate their robustness and stability over an extended period of time.

#### 4.1.1. Sensitivity studies

A first field test was carried out using ten calibrated D-shuttle sensors (commercial version) mounted on a standard metallic waste container and with actual radioactive waste. The test was performed by measuring the dose rate in the waste container while placing nine very weakly radioactive pieces in sequence inside the container over one week. The dose rate of each piece, ranging from 250 nSv/h

[6] Apache Kafka: https://kafka.apache.org/, (accessed 22 September 2020).
[7] InfluxDB: https://www.influxdata.com/, (accessed 22 September 2020).
[8] Grafana: https://grafana.com/, (accessed 22 September 2020).

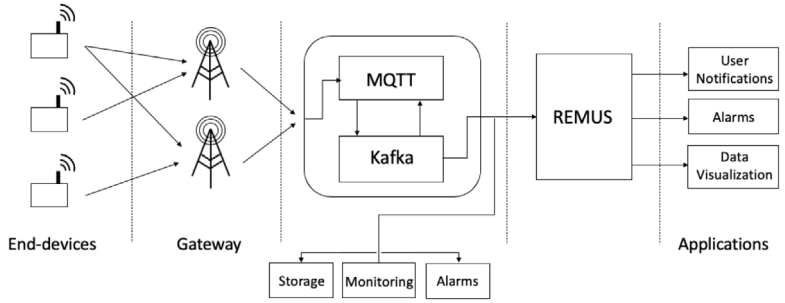


**Fig. 2.** W-MON IoT architecture.

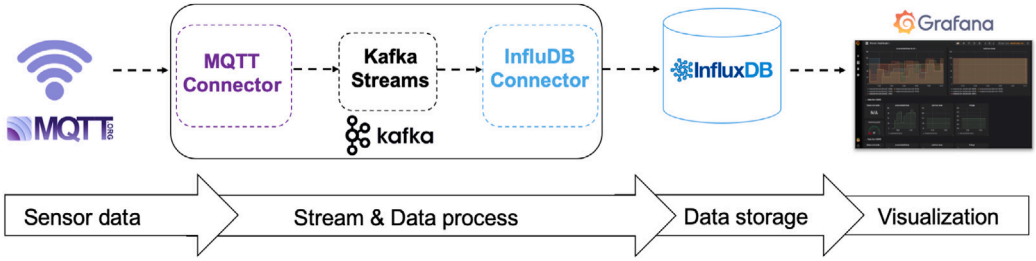


**Fig. 3.** Simplified diagram of the W-MON centralized IoT end-to-end data pipeline.


**Fig. 4.** Picture of a standard metallic container for household waste. The dimensions of the container are visible in the picture.

to 540 nSv/h, was measured in contact with a calibrated Automess 6150AD6[9] equipped with an external 6150 ADb high sensitivity gamma and X-ray probe.[10] After a piece was put inside the container, the dose rate was also measured with an Automess AD6 at four positions in contact with the waste container. These positions roughly corresponded to the four mounting positions of the D-shuttles at the centre of the side walls but 10 cm lower (closer to the bottom of the container).

The waste used for this test was metallic material activated in proton accelerators, which position in the accelerators as well as the irradiation and decay times are not known. Therefore, the exact radionuclide inventory of the nine pieces is undefined. Typical radionuclides produced in this type of activated metals are Co-60, Na-22, Mn-54, etc, with an averaged photon energy of the order of 1 MeV (Thomas and Stevenson, 1988; Magistris et al., 2018). According to the manufacturer, the energy range of the D-Shuttle is in the range between 60 keV to 1.25 MeV and therefore, it is well suited for this kind of measurements.

During the test, two configurations were studied (Fig. 5). In the first configuration, two sensors were placed at the bottom (mounted outside the container), in a central position; four sensors at mid height on the side walls and four sensors on the lid. In the second configuration, two sensors were moved from the lid to the bottom. Fig. 6 shows the dose rate versus time for the ten sensors. As expected, the sensitivity is dominated by the geometry and the sensors at the bottom turned out to be significantly the most sensitive as the samples were placed at the bottom of the container. The sensors on the side walls measured an increased dose rate (see the left hand side of Fig. 6), while the sensors on the lid did not detect any deviation from background due to the large distance from the radioactive samples. The average reading of the four side-mounted sensors is compatible with the dose rate measured by the calibrated Automess AD6 in contact with the waste container.

Results from this test demonstrate that the D-shuttle, with a sensitivity of 10 counts per 100 nSv, was able to measure dose rate variations inside a standard container for household waste from actual radioactive waste. It should be noted that for our purpose, it is sufficient to detect count rate variations from background over a time scale of one hour.

#### 4.1.2. Environmental dose rate monitoring

Fig. 7 shows the dose rate versus time for eight calibrated commercial D-shuttles mounted on a waste container for seven months (April–October 2017). The container was placed outdoors and emptied once a week through the regular garbage collection procedure. Two sensors were placed at the bottom in a central position and outside the container, two on the lid in a central position and four at mid-height on the side walls.

The dose rate in Fig. 7 was averaged at each position (from top to bottom: lid, mid-height, and bottom). Results show that the background rate is rather constant (average value ~0.07 μSv/h) with a stable behaviour of the eight sensors over the seven month test period. A peak in the dose rate was observed on the 11th of April 2017 as seen in Fig. 8. This event lasted about two hours and was identified as an industrial radiography in a nearby building. The D-shuttles were exposed to severe temperature fluctuations without showing significant

[9] Automess 6150AD6: https://www.automess.com/Download/Prospekt_ADb_E.pdf, (accessed 22 June 2020).

[10] Scintillator probe 6150AD-b: https://www.automess.de/assets/documents/en/Prospekt_ADb_E.pdf, (accessed 22 June 2020).

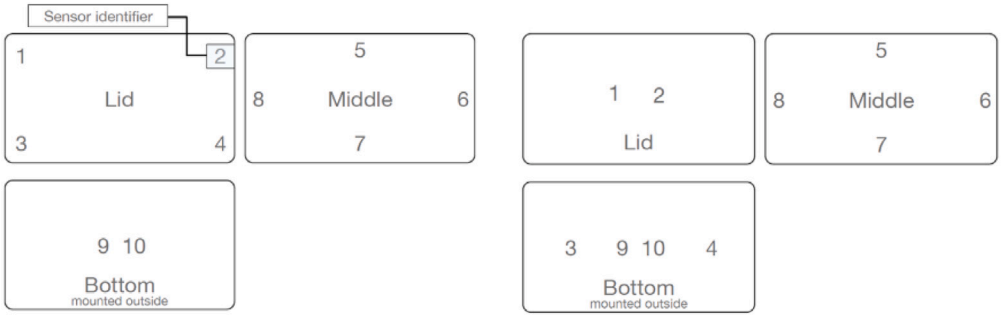


**Fig. 5.** The two tested geometrical arrangements for a 10-sensor configuration. Left: four sensors at the four corners of the lid, four at the centre of the four side walls, two on the bottom. Right: two sensors on the lid, four at the centre of the four side walls, four on the bottom.

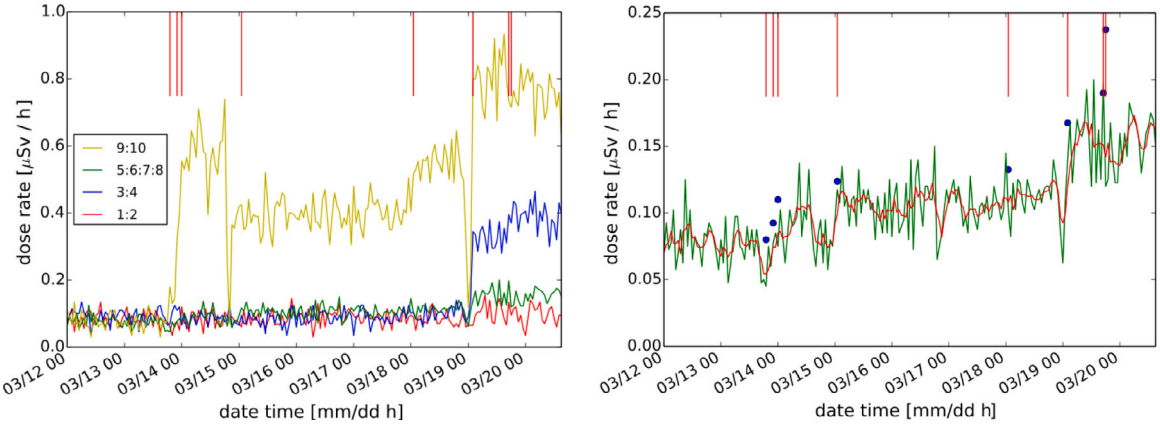


**Fig. 6.** On the left, summary plot of the dose rate measured during the field test. The vertical red lines indicate when a radioactive piece was inserted in the waste container. Sensors 1 and 2 were placed on the lid, 5 to 8 at mid height on the side walls and 9 to 10 at the bottom. Sensors 3 and 4 were initially placed on the lid and later moved to the bottom of the container. On the right, zoom on the average reading of the four side-mounted sensors. The blue dots show the average of the activity measured with the Automess AD6 in contact with the waste container. (For interpretation of the references to colour in this figure legend, the reader is referred to the web version of this article.)

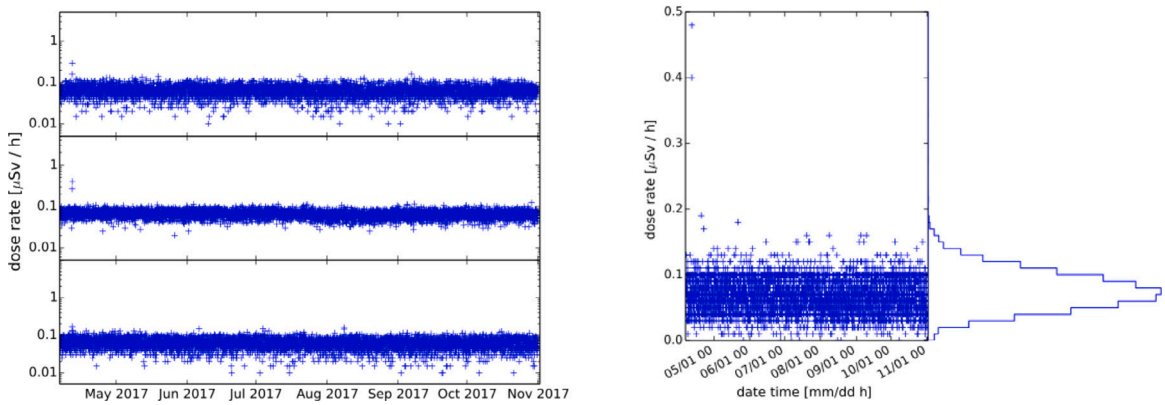


**Fig. 7.** On the left, time series of the dose rate (average value for a given position on the container) for the seven months test. From top to bottom: sensors on the lid, sensors on the side walls and sensors at the bottom. The average value of the background is ~0.07 μSv/h. On the right, time series and histogram of the dose rate for one of the devices mounted on the side walls.

variations in the dose readings. Based on the historical weather data for 2017 in the Geneva region (see Geneva forecast, 2017), the container was exposed to temperature variations from −4 °C to 30 °C, with peaks exceeding 40 °C inside the container and with significant precipitations throughout the entire duration of the test.

The hourly dose information provided by the D-shuttle has been useful to estimate the background radiation level over a long period of time. The calculated mean background hourly dose rate is 0.07 ± 0.03 μSv/h. This value is in good agreement with the results reported for the D-shuttle by other authors (Musto et al., 2019). Fig. 9 shows the dose rate distribution for one of the devices mounted on the side wall at mid-height. The count rate was calculated assuming 10 counts per 100 nSv (see right hand side of Fig. 9). Data follows a Poisson distribution with a mean value of 7 counts per hour, which corresponds to an uncertainty of around 38%. These results have been used to evaluate the minimum detectable signal and the probability of false alarm (see Section 4.3).

### 4.2. Laboratory calibration

The customized version of the D-shuttle, the BG51, and the NI-RM02 were calibrated in the CERN Radiation Calibration Facility (Pozzi et al.,

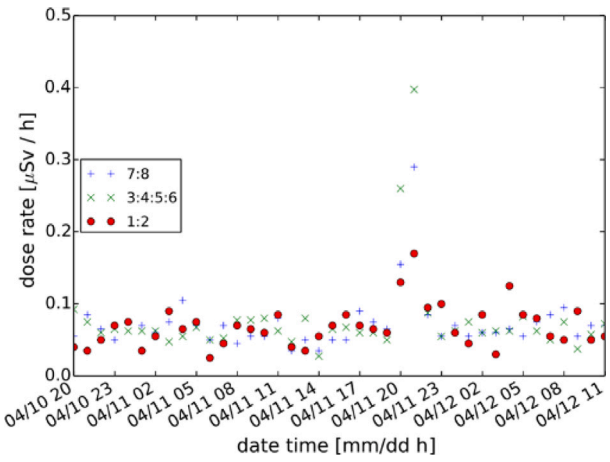


**Fig. 8.** Zoom on the dose rate during the test, averaged for a given position on the container (sensors 1:2 on the lid, 3:4:5:6 on the side walls and 7:8 at the bottom). A nearly two-hour event was observed on the 11th of April 2017 due to an industrial radiography in a nearby building.

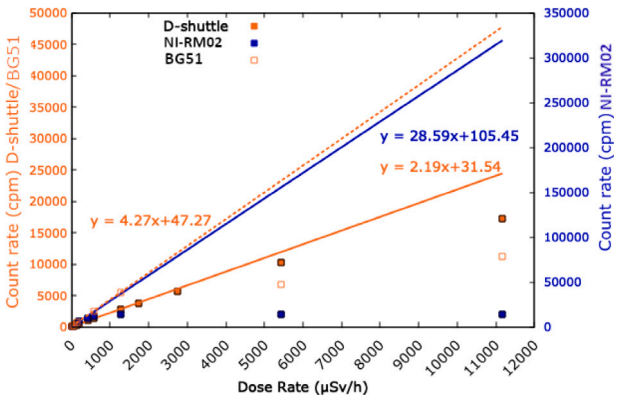


**Fig. 10.** Calibration curves obtained for the three dosimeters with Cs-137 sources up to a maximum dose rate of 11.1 mSv/h. The lines represent the linear fit to the measured data up to 2 mSv/h for D-shuttle (solid orange line, left Y-axis) and BG51 (dashed orange line, left Y-axis) and 300 μSv/h for NI-RM02 (solid blue line, right Y-axis). (For interpretation of the references to colour in this figure legend, the reader is referred to the web version of this article.)

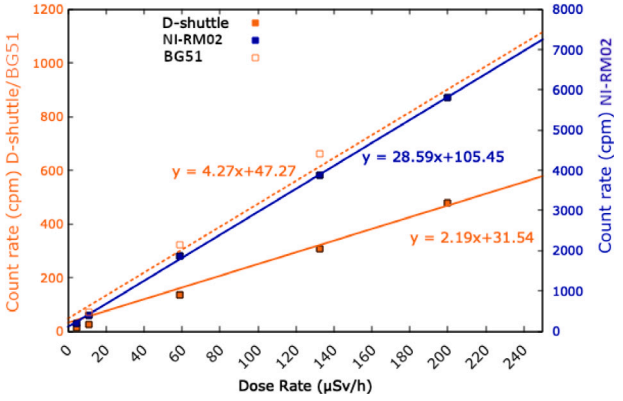


**Fig. 11.** Zoom of the calibration curves obtained for the three dosimeters with Cs-137 sources up to a maximum dose rate of 250 μSv/h. The lines represent the linear fit to the measured data for D-shuttle (solid orange line, left Y-axis), BG51 (dashed orange line, left Y-axis) and NI-RM02 (solid blue line, right Y-axis). (For interpretation of the references to colour in this figure legend, the reader is referred to the web version of this article.)

2017; Pozzi, 2016). A gamma source irradiator provides a collimated photon beam. Five Cs-137 sources with activities of 3 TBq, 300 GBq, 30 GBq, 3 GBq, and 300 MBq are available to provide ambient dose equivalent rates, $H^*(10)$, from a few μSv/h to hundreds of mSv/h. The dose rate can also be modified by changing the distance between the source and the detector.

Figs. 10 and 11 show the comparison between the three calibrated dosimeters. The results show significant variations in sensor sensitivity, ranging from 36 counts/nSv to 476 counts/nSv. The measured sensitivities of the D-shuttle and BG51 are in good agreement with the specifications, whereas the sensitivity of the NI-RM02 sensor is about a factor of 2 lower than expected (see Table 2). The differences in the sensor response values are consistent with the differences among the sensor areas (see Table 3). As expected, the dosimeter from Nuclear Instruments is more sensitive compared to the other two sensors, but it exhibits a noticeable saturation at around 300 μSv/h. The saturation for the D-shuttle and BG51 sensors is observed at around 3 and 2 mSv/h respectively. Saturation is not important for our specific application but has been studied to check the overall performance of each sensor. Based on the above results, all dosimeters are sensitive enough to discriminate radiation levels above the natural background.

### 4.3. Detectability strategy and sensor arrangement

The number of radiation sensors as well as their distribution inside the waste container is an important aspect of the project. As shown above, the sensitivity of the system is dominated by its geometry, depending on the number of sensors and on the distance between them and the radioactive source (see Section 4.1.1). A simulation was performed in order to optimize the number of devices and determine the best geometrical arrangement in a way that minimizes this distance.

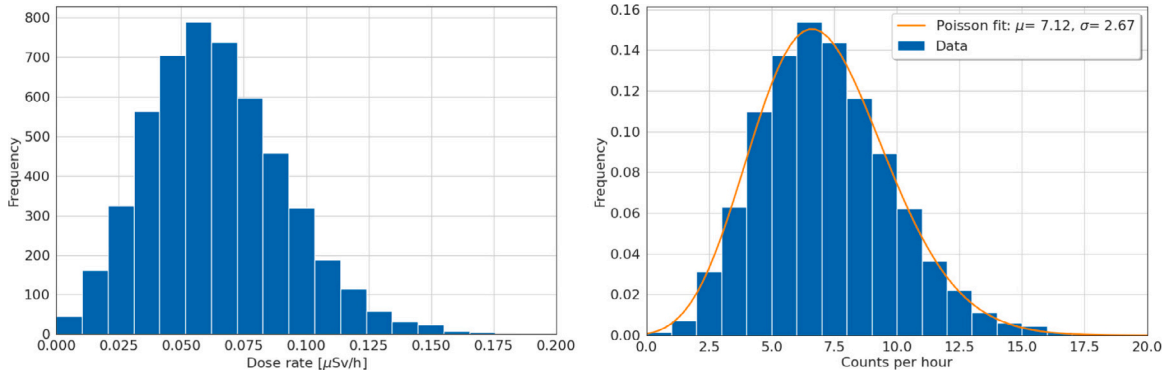


**Fig. 9.** On the left: histogram of the dose rate for one of the devices mounted on the side walls. On the right: histogram of the count rate assuming 10 counts per 100 nSv as reported by the manufacturer. The solid orange line represents a Poisson fit to the data.

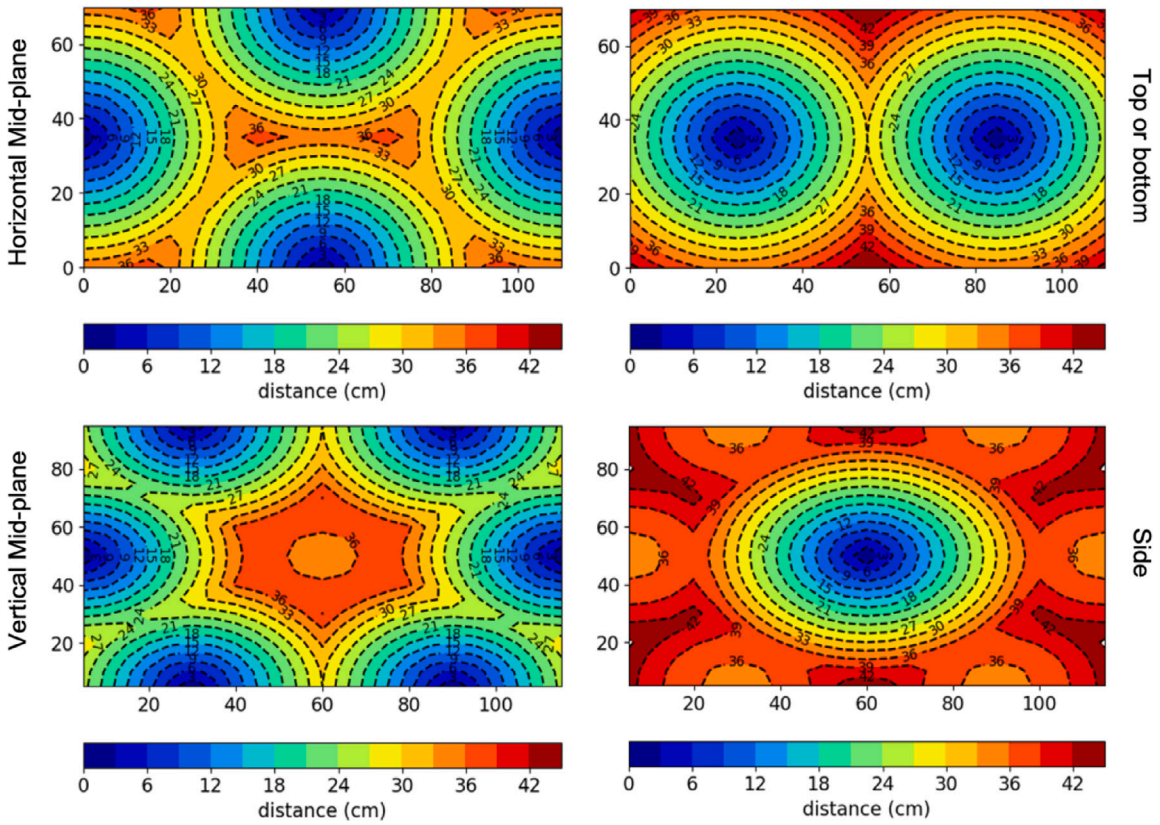


**Fig. 12.** Various cross sections of the 3D map of the distance to the closest sensor for a configuration with eight D-shuttles. The values on the X and Y axis are the container dimensions in centimetres.

**Table 3**
Comparison between the three radiation sensors.

| | Pulse count rate (cpm for 1 μSv/h) | Saturation (μSv/h) | Sensor size ($mm^2$) | Count rate per sensor surface (cpm/$mm^2$ for 1 μSv/h) |
|---|---|---|---|---|
| NI-RM02 | 28.59 | 300 | 100 | 0.28 |
| BG51 | 4.27 | 2000 | 15.5 | 0.28 |
| D-shuttle | 2.19 | 3000 | 7.29 | 0.28 |

For this study, environmental background measurements with the three sensors (customized D-shuttle, BG51, and NI-RM02) were used. The mean hourly dose of the three dosimeters as well as the uncertainty were estimated over a period of several weeks. The mean natural background level at CERN is around 100 nSv/h. The calculated background rate of the sensors is: 10 counts/h (D-shuttle), 30 counts/h (BG51), and 150 counts/h (NI-RM02) with fluctuations of 30%, 18%, and 10%, respectively.

The waste container was modelled as a box of 110 cm × 70 cm × 90 cm (see Fig. 4). A raster scan of the volume of the container divided in cubic voxels of 5 cm × 5 cm × 5 cm was performed using Python (Rossum and Drake, 2009), generating a map of the distance between any point inside the container and its closest sensor. Fig. 12 shows 2D sections of these maps for a configuration with eight sensors; two at the bottom, four at the centre of the side walls and two on the lid. The fraction of the container's volume at a distance x ± $\epsilon$ (where $\epsilon$ accounts for the distance variations from each sensor to the different points inside a voxel) and the percentage of the volume at less than a certain distance are shown on the left and right hand sides of Fig. 13 respectively, both from the closest sensor. In this case, the volume of the box was divided in cubic voxels of 1 cm × 1 cm × 1 cm. The median value of the distance to the closest sensor is 27.6 cm, with less than 2% of the volume at more than 40 cm.

For any position inside the container, we can calculate the average expected count rate for each sensor for a given radioactive source activity. The left hand side of Fig. 14 shows the fraction of the volume from where the closest sensor detects a certain count rate from a 90 kBq Cs-137 source (the activity of the source was chosen arbitrarily). For this example, we used the D-shuttle dosimeter. The expected background rate was 10 counts/h, with 30% fluctuation on a single measurement. Unsurprisingly, the sensors measure low count rates, with only 15.5% of the volume producing a count rate greater than twice the background (20 counts/h) at least in one sensor. This is more clear on the right hand side of Fig. 14. In what follows, the probability of detecting a source by one or more sensors (depending on the trigger mode as explained below) will be assessed by the fraction of the container's volume covered by such sensor(s) with a count rate higher than a certain threshold.

The protocol to detect radioactivity inside the container can be based on an individual triggering, i.e. each sensor applies an individual threshold over the detected signal and triggers an alarm when this threshold is exceeded, regardless of the signal detected by the other sensors. Another approach can be based on a combined triggering method, where the signals from more than one sensor are considered (i.e. added up) to provide a new triggering level. In either case, the Minimum Detectable Signal (MDS) needs to be defined.

A commonly accepted critical level ($L_c$) is set in such a way that, in absence of radioactivity, the probability of a false positive or Probability of False Alarm (PFA) is no greater than 5% (Currie, 1968; Knoll, 2000; Weise et al., 2005). As shown in Section 4.1.2, for the D-shuttle, the background hourly counts follow a Poisson distribution. Therefore, for a PFA of 5% and an integration time of one hour, the D-shuttle's MDS can be set at 15 counts (5 counts above background). However, this implies that, in the absence of radioactivity, 5% of the time the background would be incorrectly identified as a signal resulting in an unacceptable number of false positives for a W-MON type system

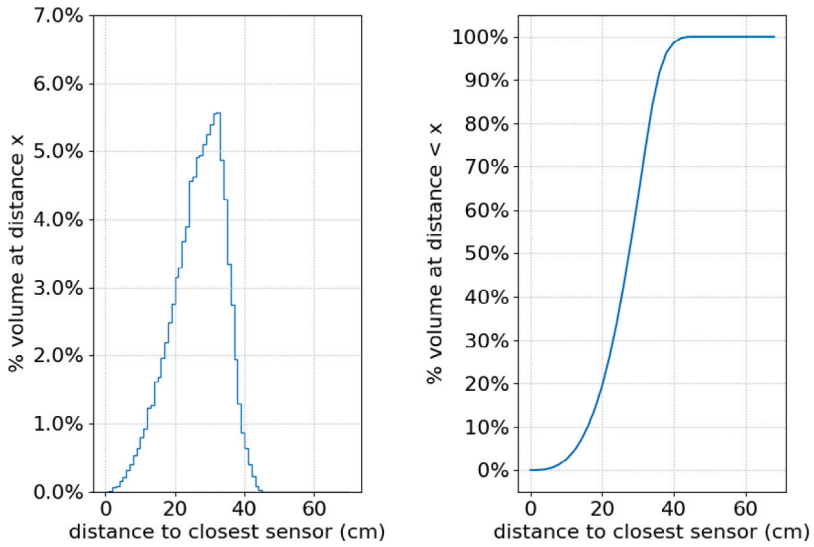


**Fig. 13.** On the left, fraction of the container's volume at a distance x ± $\epsilon$ from the closest sensor for the configuration with eight sensors described in the text. On the right, percentage of the volume at less than a distance x ± $\epsilon$ to the closest sensor.

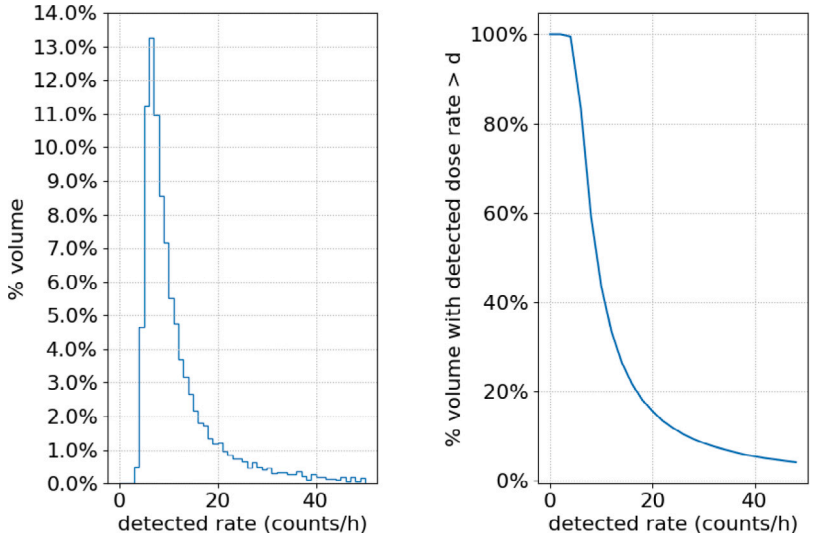


**Fig. 14.** On the left, expected count rate for a Cs-137 source with 90 kBq activity, moved inside the box on a 3D grid. As a reference, the expected rate for background is 10 counts/hour. On the right, fraction of the container's volume from which the source will lead to a count rate higher than a certain value $d$ in the closest sensor.

where an intervention will take place every time an alarm is triggered. Higher detectability limits can be established to reduce the number of false positives. For example, for a MDS at 3 standard deviations above background (19 counts) (McLaughlin, 1973), the PFA will only be of the order of 0.35%. However, it should be noted that higher thresholds will also affect the detection capability for low activity items.

More complex approaches can be adopted in order to reduce the PFA while keeping the MDS reasonably low. For example, one can vary the number of consecutive positive signals required to trigger an alarm. For instance, the system could ask for two consecutive hourly measurements above a MDS defined for a PFA of 5% before triggering an alarm. In this way, the PFA will significantly decrease from 5% to 0.25%. The PFA can be further improved by increasing the time difference between the first trigger and the final alarm. This method has the advantage of improving the detectability performance of the system while keeping an hourly granularity.

A combined trigger method can help improve the monitoring capabilities of the system. By aggregating several sensors, the number of background counts becomes sufficiently high such that the Poisson distribution can be approximated by a Gaussian distribution. This is valid for the three types of sensors. Therefore, assuming no correlation between devices, the mean value of the background for a system with $N$ sensors is defined as the sum of the mean values of each individual sensor. The variance can be calculated as the sum of the variance of each sensor

$$\sigma_N^2 = \sum_{i=1}^{N} \sigma_i^2, \tag{1}$$

where $\sigma_i$ is the standard deviation of the background signal of the sensor $i$. Following the same approach as before, one could set an MDS in such a way that the PFA is no greater than 5% for the standard deviation of the background counts given by Eq. (1).

In this section we present, as example, the results of the simulation for the D-shuttle and a 90 kBq Cs-137 source moved inside the box on a 3D grid for two extreme detection limits: an MDS equal to $L_c$ (5% nominal significance level) and at $3{\cdot}\sigma_N$ above background. It should be stressed that this study does not intend to provide a value for the detection limit but to explain the potential of a system with the characteristics of W-MON and to determine the optimal configuration of sensors in the waste container on a sensitivity basis. A radiological

**Table 4**
Detection probability of a 90 kBq Cs-137 source using different combinations of closest sensors and two different threshold levels. The study was done with eight D-shuttles with a sensitivity of "10 counts for a dose of 100 nSv", 30% fluctuation on a single measurement and one hour integration time.

| Number of sensors | | 1 | 2 | 3 | 4 | 5 | 8 |
|---|---|---|---|---|---|---|---|
| Detection probability | $L_c$ | 91.5% | 98.8% | 99.2% | 99.5% | 99.1% | 98.2% |
| | $3{\cdot}\sigma_N$ | 51.4% | 57.1% | 59.0% | 62.0% | 60.3% | 46.2% |

**Table 5**
Fraction of the volume with a count rate higher than $L_c$ measured by different combinations of closest sensors to a 90 kBq Cs-137 source, for different configuration with six, eight and ten D-shuttles per container.

| Number of sensors per container | Median distance to the closest sensor [cm] | % volume with total detected count rate ≥ $L_c$ | | | | | | | |
|---|---|---|---|---|---|---|---|---|---|
| | | Number of closest sensors | | | | | | | |
| | | 1 | 2 | 3 | 4 | 5 | 6 | 8 | 10 |
| Six | 30.27 | 78.6 | 89.1 | 89.3 | 90.3 | 89.0 | 87.6 | – | – |
| Eight | 27.6 | 91.5 | 98.8 | 99.2 | 99.5 | 99.1 | 99.2 | 98.2 | – |
| Ten | 25.54 | 93.3 | 99.3 | 99.8 | 100.0 | 99.9 | 99.9 | 99.8 | 99.7 |

classification limit of potentially radioactive waste based on dose rate measurements would require additional studies that must include a representative sample of items with different characteristics (materials, activities, dimensions, masses, etc.) (Frosio et al., 2020).

Fig. 15 shows the fraction of the container's volume with an expected count rate higher than a certain value $d$ for various combinations of sensors (based on single- and combined-trigger modes) assuming a configuration of eight D-shuttles per container. The dashed lines represent the MDS equal to $L_c$. For background levels below 30 counts (one, two and three D-shuttles), the $L_c$ was calculated using Poisson statistics. For a configuration with four or more sensors a normal distribution is applicable. The results are summarized in Table 4. For this specific case, the combination of the four closest sensors to a Cs-137 source with an activity of 90 kBq provides the best coverage of the volume with a fraction of 99.5%. A higher number of sensors does not increase the probability of detecting the source as might be expected, because the resulting increase in noise contribution is more significant than the signal increase. Similar results were obtained for a MDS set at 3 standard deviations above background (see Supplementary material). The probability of detecting the source increased to up to 62% with a combination of four sensors (see Table 4). No further improvement was observed when all eight sensors were added up. It is also clear that if we increase the detection level, the probability of detecting the source decreases impairing the system performance. In what follows, a minimum detectable signal equal to $L_c$ has been chosen.

To decide the minimum number of sensors that, properly arranged around the waste container, will provide the desired sensitivity, we tested several configurations for six, eight, and ten devices per container. The results reported in this paper only refer to the best setting for each of the tested configurations. The results reported in Table 5 show that, as the number of devices per container increases, the median value of the distance to the closest sensor decreases and reduces from 30.27 cm with six sensors to 25.54 cm with ten, increasing the detection probability. The best detection efficiency provided by a configuration of six sensors, assuming a combined triggering mode and a MDS equal to $L_c$, is 90.3%, i.e. 9.2% lower than for a set-up with eight devices. On the other hand, ten sensors strategically distributed around the container would increase the detection effectiveness of less than 1% compared to a configuration with eight sensors, which does not justify the cost for two additional sensors. These results depend, in addition to the threshold level, on the activity of the object. For a minimum detectable signal equal to $L_c$ and activities up to 150 kBq, the difference between the best detection efficiencies obtained for an 8-sensor and a 10-sensor configurations is in average below 5% with a maximum

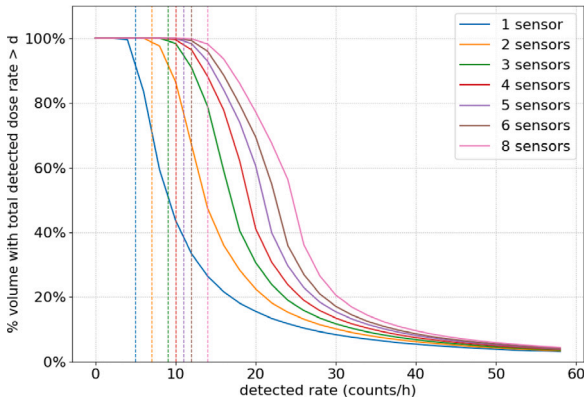


**Fig. 15.** Detection probability of a 90 kBq Cs-137 source using different combinations of closest sensors for a configuration with eight D-shuttles with a sensitivity of "10 counts for a dose of 100 nSv", 30% fluctuation on a single measurement and an integration time of one hour. The dashed lines indicate the value of the minimum detectable signal, equal to $L_c$. (For interpretation of the references to colour in this figure legend, the reader is referred to the web version of this article.)

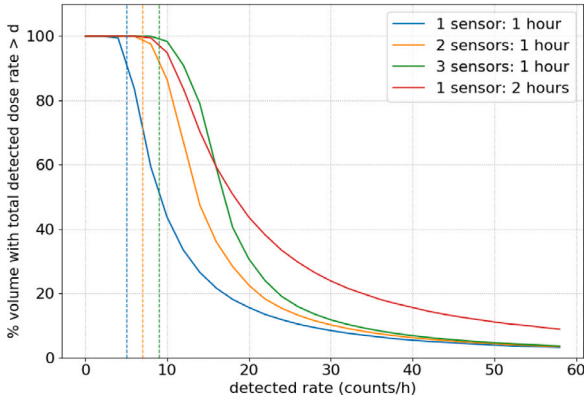


**Fig. 16.** Detection probability of a 90 kBq Cs-137 source using different combinations of closest sensors for a configuration with eight D-shuttles and two different integration times. The dashed lines indicate the value of the minimum detectable signal equal to $L_c$. The threshold level for two hours integration time is equal to that of the two closest sensors and one hour integration time. (For interpretation of the references to colour in this figure legend, the reader is referred to the web version of this article.)

of the order of 15% for a 40 kBq Cs-137 source. As for the PFA, the detection probability can be improved by increasing the time difference between a first positive signal and an alarm. The results show that the gain obtained by arranging ten sensors in the container can be easily matched with an 8-sensor configuration by waiting one hour more before triggering the alarm, reducing overall cost of the system (see Fig. 16). Since garbage is collected twice or three times per week, on average, an additional hour waiting for a confirmation before an alarm is triggered does not represent a major drawback. This amelioration is less important on a configuration with 6-sensors due to the greater distance between the sensors and the source.

Similar analyses have been carried out for the BG51 and NI-RM02 radiation sensors. The sensitivity in counts and the statistical uncertainties at background level were estimated over a time period of several weeks. For an 8-sensor configuration, Fig. 17 compares the expected count rate measured by the closest sensor for a 50 kBq Cs-137 source using the three type of sensors. The dashed lines indicate the MDS equal to $L_c$ for each sensor. As expected, higher sensitivities provide better coverage of the container's volume for the same dose rate. As for the D-shuttle, in certain cases, a combined trigger model also improves the detection performance of a system based on the BG51 and NI-RM02. The difference between the best detection efficiencies obtained for an

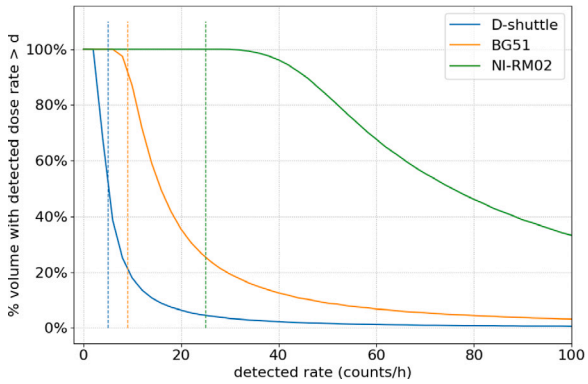


**Fig. 17.** Fraction of volume with a given count rate from a 50 kBq Cs-137 source higher than a certain value *d* measured by the closest sensors for an 8-sensor configuration. Results are shown for the D-shuttle, BG51 and NI-RM02. The dashed lines indicate the value of the minimum detectable signal equal to $L_c$. (For interpretation of the references to colour in this figure legend, the reader is referred to the web version of this article.)

8-sensor and a 10-sensor configurations is, in average, below 3% for both types of sensors.

Based on the sensitivity studies performed with a wide range of activities of a Cs-137 source, an array of eight sensors per container with two at the bottom, four at the centre of the side walls and two on the lid is optimal to provide full coverage of the inner volume ensuring cost-effectiveness. Nonetheless, the final strategy will depend on the actual frequency of occurrence of radioactive objects. The foreseen field tests using a large number of typical items found in waste containers may therefore reveal the need for a different configuration of sensors. We have shown that by combining the signals from different sensors and increasing the total integration time, the risk of false alarms can be minimized while the detection probability, which is critical for low activity items, can be increased.

## 5. Conclusions

This paper describes an interconnected network of radiation sensors for environmental radiological monitoring based on customized radiation monitoring devices. Extensive tests have been performed using the D-shuttle personal dosimeter mounted on a regular-used metallic container for conventional waste and weakly radioactive material. These tests have served both to study the performance of the D-shuttle and as proof-of-concept for the W-MON project. The sensitivity of the D-shuttle sensor is sufficiently high to measure dose rate variations inside a standard waste container from actual radioactive waste. Background measurements over an extended period of time of seven months showed that the D-shuttle is suitable for stable low-dose rate radiation measurements with a mean hourly dose of $0.07 \pm 0.03$ μSv/h. However, none of the two independent communication interfaces offered by the D-shuttle allowed for long-range data transmission.

The requirements of the W-MON project in terms of low-power and long-range wireless data transmission required the development of a dedicated communication board with custom-designed hardware and software, and a radiation sensor with similar characteristics of those of the D-shuttle but easy to couple to the communication board. Three suitable options for the radiation sensor have been described in this paper. The sensors have been tested with a custom-made communication board allowing for LoRa wireless data transmission. Currently, radiation measurements are successfully and periodically sent to the CERN LoRaWAN network connected to a robust and reliable monitoring architecture with customized user dashboards for real-time visualization and status control of the devices. Several tests have been performed to verify the technical characteristics of the three candidate sensors. A dedicated simulation has been carried out to evaluate the distribution of the dosimeters around the container and their monitoring capabilities as a function of the sensor's sensitivity. The chosen system architecture is based on an array of eight radiation sensors per waste container, providing a full coverage of the inner volume with the required sensitivity while ensuring cost-effectiveness. In order to conclude which sensor suits best the requirements of W-MON, tests under realistic conditions using actual radioactive waste are foreseen. The scope of the tests is to evaluate the performance of the three dosimeters over a long time period (around six months) in terms of sensitivity, power consumption, data transmission efficiency, robustness, stability, and reliability. Additionally, these tests will allow us to establish the detection limit for the radiological classification of potentially radioactive items and to implement the detection criteria based on a combined trigger mode into REMUS.

It is worth mentioning that a W-MON type system can find a wide range of applications. Its versatility makes it very attractive as a wireless personal dosimetry system that can be used, for example, for on-line monitoring of the dose received by medical staff during interventional radiology procedures. Additionally, a distributed system with centralized intelligence such as W-MON may be an attractive option for environmental monitoring of large areas, offering continuous monitoring of the environmental gamma dose with high granularity and therefore, overcoming the limitations posed by the use of passive dosimeters. A wireless radiation sensor such as the ones discussed in this paper, equipped with a GPS module, can provide real-time dose data alongside location information being useful, for example, for the tracking of radioactive sources or activated equipment on fixed or mobile platforms.

## Declaration of competing interest

The authors declare that they have no known competing financial interests or personal relationships that could have appeared to influence the work reported in this paper.

## Acknowledgements

The authors would like to thank Dr Suzuki (AIST) for his contribution in the development of the new version of the D-shuttle radiation sensor and the CERN IT group for the technical guidance and assistance.

## Appendix A. Supplementary data

Supplementary material related to this article can be found online at https://doi.org/10.1016/j.radmeas.2020.106488.

## References

Adachi, N., Adamovitch, V., Adjovi, Y., Aida, K., Akamatsu, H., Akiyama, S., Akli, A., Ando, A., Andrault, T., Antonietti, H., Anzai, S., Arkoun, G., Avenoso, C., Ayrault, D., Banasiewicz, M., Banaśkiewicz, M., Bernandini, L., Bernard, E., Berthet, E., Zuclarelli, E., 2015. Measurement and comparison of individual external doses of high-school students living in Japan, France, Poland and Belarus - the "D-shuttle" project. J. Radiol. Prot. 36, 49–66.

Augustin, A., Yi, J., Clausen, T., Townsley, W.M., 2016. A study of LoRa: Long range & low power networks for the Internet of Things. Sensors 16, 1466.

Bezerra, N.S., Åhlund, C., Saguna, S., de Sousa, V.A., 2019. Propagation model evaluation for LoRaWAN: Planning tool versus real case scenario. In: 2019 IEEE 5th World Forum on Internet of Things (WF-IoT). pp. 1–6.

Cemusová, Z., Ekendahl, D., Judas, L., 2017. Testing of the D-shuttle personal dosemeter. Radiat. Meas. 106, 214–217, Proceedings of the 18th International Conference on Solid State Dosimetry (SSD18), Munich, Germany, 3 – 8 July 2016.

Currie, L.A., 1968. Limits for qualitative detection and quantitative determination. application to radiochemistry. Anal. Chem. 3 (40), 586–593.

Frosio, T., Dumont, G., Froeschl, R., Iliopoulou, E., Magistris, M., Menaa, N., Roesler, S., Theis, C., Vincke, H., Vincke, H., 2020. Classification of radiological objects at the exit of accelerators with a dose-rate constraint. Appl. Radiat. Isot. 165, 109303.

Geneva forecast, 2017. Prevision Meteo. https://www.prevision-meteo.ch/climat/mensuel/geneve-cointrin/2017, (accessed 28 September 2020).

Gnawali, O., Fonseca, R., Jamieson, K., Moss, D., Levis, P., 2016. Demystifying low-power wide-area communications for city IoT applications.

Islam, S., Watanuki, S., Tashiro, M., Watabe, H., 2019. Error evaluation of the D-shuttle dosimeter technique in positron emission tomography study. Radiol. Phys. Technol. 12.

Kim, D., Murayama, K., Nurtazin, Y., Koguchi, Y., Kenzhin, Y., Kawamura, H., 2019. Intercomparison exercise at Harshaw 6600, DVG-02TM, and D-shuttle dosimeters for the individual monitoring of Ionizing Radiation. J. Radiat. Prot. Res. 44, 79–88.

Knoll, G.F., 2000. Radiation Detection and Measurement, third ed. Wiley, New York, NY.

Ledeul, A., Segura, G., Silvola, R.P., Styczen, B., Vasques, D.R., REMUS: the new CERN radiation and environment monitoring unified supervision. In: ICALEPCS2015. Melbourne, Australia.

LoRa Alliance, 2020. https://lora-alliance.org/about-lorawan, (accessed 20 April 2020).

Magistris, M., Frosio, T., Theis, C., Ulrici, L., Zaffora, B., 2018. Radiological characterization of very-low-level radioactive waste at CERN. In: DEM 2018: International Conference on Dismantling Challenges: Industrial Reality, Prospects and Feedback Experience.

McLaughlin, J.E., 1973. Measurement of low-level radioactivity, icru-22. Nucl. Sci. Eng. 50 (2), 184.

Moyer, B., 2015. Low power, wide area: A survey of longer-range IoT wireless protocols. Electron. Eng. J. (accessed 22 September 2020).

Musto, E., Assenmacher, F., Hofstetter-Boillat, B., Mayer, S., Yukihara, E., 2019. Use of the D-shuttle dosimeter for radiation protection of members of the public: Characterization and feasibility study. Radiat. Meas. 129, 106208.

Naito, W., Uesaka, M., Yamada, C., Kurosawa, T., Yasutaka, T., Ishii, H., 2016. Relationship between individual external doses, ambient dose rates and individuals' activity-patterns in affected areas in fukushima following the fukushima daiichi nuclear power plant accident. PLOS ONE 11 (8), 1–12.

Petäjäjärvi, J., Mikhaylov, K., Pettissalo, M., Janhunen, J., Iinatti, J., 2017. Performance of a low-power wide-area network based on LoRa technology: Doppler robustness, scalability, and coverage. Int. J. Distrib. Sens. Netw. Vol. 13, 1–16.

Pozzi, F., 2016. CERN Radiation Protection (RP) Calibration Facilities (PhD thesis). Technischen Universität München.

Pozzi, F., Alia, R.G., Brugger, M., Carbonez, P., Danzeca, S., Gkotse, B., Jaekel, M.-R., Ravotti, F., Silari, M., Tali, M., 2017. CERN irradiation facilities. Radiat. Prot. Dosim. 180, 120–124.

Raza, U., Kulkarni, P., Sooriyabandara, M., 2017. Low power wide area networks: An overview. In: IEEE Commun. Surv. Tutor., Vol. 19. pp. 855–873.

Rossum, G.V., Drake, F., 2009. Python 3 Reference Manual.

Sierra, R., 2019. Put a sensor in your life with the new LoRaWAN network. In: Bulletin for the CERN Community, Issue No. 5-6/2019.

Thomas, R.H., Stevenson, G.R., 1988. Radiological safety aspects of the operation of proton accelerators.

Weise, K., Hübel, K., Michel, R., Rose, E., Schläger, M., Schrammel, D., Täschner, M., 2005. Determination of the Detection Limit and Decision Threshold for Ionizing-Radiation Measurements: Fundamentals and Particular Applications. TÜV Verlag Rheinland, Köln, ISSN 1013-4506, ISBN 3-8249-0945-6, FS-05-129-AKSIGMA.